Regular Article

PHYSICAL CHEMISTRY RESEARCH
Published by the
Iranian Chemical Society
www.physchemres.org
info@physchemres.org

Phys. Chem. Res., Vol. 8, No. 2, 225-240, June 2020
DOI: 10.22036/pcr.2020.208780.1700

Adsorption and Removal Characterization of Nitrobenzene by Graphene Oxide Coated by Polythiophene Nanoparticles

S.M. Mousavi[a], A. Babapoor[b], S.A. Hashemi[a] and B. Medi[c,*]

[a]*Department of Medical Nanotechnology, School of Advanced Medical Sciences and Technologies, Shiraz University of Medical Sciences, Shiraz, Iran*

[b]*Department of Chemical Engineering, University of Mohaghegh Ardabili, P. O. Box: 179, Ardabil, Iran*

[c]*Department of Chemical Engineering, Hamedan University of Technology, P. O. Box: 65155-579, Hamedan, Iran*

(Received 16 November 2019, Accepted 18 January 2020)

Nitrobenzene (NB) has a wide range of usage as a chemical intermediate and also as a dye in printing applications. Despite its advantages, NB is harmful to human and animals and hence is an environmental pollutant. In this research, NB removal from water was studied *via* adsorption on graphene oxide (GO) coated by polythiophene (PT) nanoparticles. The resulting nanocomposite was characterized by XRD, FTIR, BET and SEM. While the FTIR tests proved successful incorporation of PT, the SEM images displayed a relatively larger surface area compared to the other studies. The BET analysis confirms this finding by reporting the surface area as 917.8 m^2 g^{-1} for the adsorbent. The adsorption mechanism was assessed by the Langmuir and Freundlich isotherms. The results show that the Freundlich isotherm better describes the adsorption process compared to the Langmuir isotherm. On the other hand, the pseudo-second-order kinetic model better regresses the experimental results, which indicates a chemical adsorption mechanism. The adsorption-desorption behavior of the samples was evaluated at optimized pH, time, adsorbent dosage, and eluent type. The results showed that the synthesized nanocomposite can efficiently remove NB from solutions in the pH range of 5.0-7.0, with the maximum adsorption capacity of 15.6 m^2 g^{-1}.

Keywords: Nitrobenzene, Graphene oxide, Polythiophene, Adsorption

INTRODUCTION

Nitrobenzene (NB) is an important industrial material, which is widely used in the production of dyes, inks, explosives, and pesticides. Nevertheless, NB is an extremely toxic chemical, which is harmful to human health [1] and affects animals' reproductive system upon exposure [2]. NB is also an environmental pollutant [3].

In recent years, with environmental and economic motivations, considerable attention has been paid on the research and development of different kinds of efficient, low-cost adsorbents [4]. Qin, *et al.* [5] investigated the adsorption of NB on CH_3-MCM-41 with respect to contact time, initial NB concentration, temperature, pH, and ionic strength. The results indicated that surface modification of MCM-41 significantly enhances its adsorption capacity for NB. Sun, *et al.* [6] suggested that pore-filling and flat-surface adsorption both contribute to the adsorption of polycyclic aromatic hydrocarbons on reduced GO with dramatic effects of conformation and aggregation of the surface on the adsorption characteristics.

Chen, *et al.* [7] reported strong adsorptive interactions of nitroaromatics onto CNTs resulting from the π-π electron donor-acceptor interactions between the nitroaromatic molecules (electron acceptors) and graphene nanosheets (electron donors) of CNTs.

Foroutan, *et al.* [8] used the Callinectes sapidus biomass as a bioadsorbent for the removal of heavy metals from real wastewater. After kinetic and equilibrium studies, they concluded that the adsorption process is fast, exothermic,

*Corresponding author. E-mail: medi@hut.ac.ir

and spontaneous, and that the proposed bioadsorbent can simultaneously adsorb several pollutants (metal ions, antibiotics, sulfate, nitrate, and ammonium).

Magnetic adsorbents have been recently used for the removal of pollutants from wastewater, particularly, where heavy metals are under consideration [9,10]. However, their application is also extended to the removal of organic matters. Shi, *et al.* [11] synthesized magnetic cellulose/ graphene oxide composite (MCGO) as a novel bioadsorbent and evaluated it with an enhanced adsorption capacity for the removal of an azo dye (methylene blue). They studied the adsorption mechanism as well as the effects of pH, adsorbent dosage, and initial dye concentration with the maximum adsorption capacity, 70.03 mg g^{-1}.

Graphene is a new member of carbon family with a hexagonally sp-hybridized and one-atom-thick layer structure with interesting physicochemical properties [12]. It can be prepared from graphite, a low-cost material [13]. Since the discovery of graphene and its derivatives, they have attracted a considerable attention due to their outstanding properties in various novel applications. In the family of graphene derivatives, graphene oxide (GO) is a single sheet form of graphite, and has the ideal 2D structure with a monolayer of carbon atoms packed into a honeycomb crystal plane. GO is typically synthesized by reacting graphite powder with strong oxidizing agents such as $KMnO_4$ in concentrated sulfuric acid, through reaction paths such as the well-known Hummer's method [14,15].

In contrast to graphene, GO has many oxygen-containing hydrophilic functional groups on the graphitic backbone in the forms of hydroxyl, epoxide, carboxyl, and carbonyl groups. These oxygen groups which protrude from its layers can bind to other molecules or ions by both electrostatic and coordinate interactions, especially the multivalent metal ions. For instance, it has been reported that GO represents a great promise as a Cu^{2+} adsorbent [14]. GO can play a role as a chemical oxidant for various cyclic polymers (*e.g.*, polythiophene, polyaniline, and polypyrrole), and diverse graphene-polymer composites can simply and rapidly be synthesized by GO as both graphene precursor and chemical oxidant with enhanced synergistic effects [16].

GO has yet another unique advantage; because of the presence of several oxygen-containing functional groups, its dispersibility in water is significantly better than other members of the carbon family [4]. When integrated with a polymer, the intriguing properties of GO result in remarkable improvements in the polymer characteristics, including better dispersibility in water.

Recent studies have also shown that GO is ideal for adsorption of dyes, while it is also useful for acting as a catalyst support due to its good mechanical strength and large surface area (2630 m^2 g^{-1}) [14,17,18].

Polythiophene (PT) has attracted considerable attention because of its good environmental stability, unique redox electrical behavior, stability in doped or neutral states, ease of synthesis, and wide range of applications in many fields. The alkyl substitution of PT modifies the electronic properties of the polymer, thereby extending its potential for industrial applications. PT or substituted PT, when combined with metal, metal oxide or a combination of both, can exhibit tailorable photocatalytic properties. In particular, GO has a functional oxygen group capable of interacting with PT or its derivatives *via* a π-π interaction between the nonpolar regions of GO and the molecular layers of PT [19].

Despite the vast scope of research on the removal and/or degradation of NB as summarized above, so far, there has been no report of its removal *via* graphene oxide combined with polythiophene nanoparticles. The primary purpose of the present study is to determine the enhancement of NB adsorption from an aqueous solution on graphene oxide coated by polythiophene nanoparticles (GOPT). In this regard, Fourier-transform infrared spectroscopy (FTIR), scanning electron microscope (SEM), Brunauer-Emmett-Teller (BET) analysis, X-ray diffraction (XRD), and spectrophotometry were utilized for characterization and analysis. The adsorption behavior of NB was studied via comparison with two isotherms. We conclude that this novel nanocomposite is an efficient adsorbent of NB, which can be used for its removal from various types of wastewater.

EXPERIMENTAL

Materials

Natural graphite flakes with an average particle size of 150 μm (purity > 98%) were supplied from Qingdao Nanshu Graphite Co., Ltd., China. Concentrated sulfuric

acid (98%), hydrochloric acid (36%), hydrogen peroxide (30%), sodium nitrate, N,N-dimethylformamide (DMF), and ethanol, purchased from Chongqing Chuandong Chemical Reagent Group, China, were of analytical reagent (A.R.) grade. Potassium permanganate (A.R.), the monomer thiophene, and NB were purchased from the Fluka Company. Phosphoric acid and sodium dodecyl sulfate (SDS) were purchased from Merck (both A.R. grade).

Preparation of the Main Solutions

0.100 g of NB dye was poured in a 1000-ml volumetric flask of distilled water (NB solution was 100 mg l^{-1}). This solution was used to produce other solutions with lower consistency. 100 ml phosphoric acid (0.1 M) was poured in a 200 ml beaker then the pH was regulated at 7.0 by adding solutions of sodium phosphoric and hydrochloric acid to prepare the phosphate buffer.

Synthesis of PT Nanoparticles

The reaction was performed in a 250 ml flask equipped with a mechanical stirrer at 50 ℃. 0.1 g SDS and 2 g thiophene were added to 60 ml of deionized water, and the mixture was stirred at 300 rpm for 20 min.

Synthesis of GOPT Nanocomposite

Graphene oxide was produced by a multi-step method. In this case, at the first step, 2 l H_2SO_4 was poured in a round-bottom flask and stirred by a magnet with simultaneous heating at 50 ℃. In the second step, 50 g $KMnO_4$ was added to the H_2SO_4 solution. Then, in the third step, 10 g graphite was slowly added to the previous suspension. Afterward, in the fourth and fifth steps, 110 ml H_3PO_4 was added to the previous step suspension, and the suspension was stirred for 72 h with simultaneous heating at 50 ℃. In the sixth step, the suspension was poured in a vacuum Erlenmeyer flask along with ice (made by deionized water). Then, in the seventh and eighth steps, 10 ml H_2O_2 was poured in the suspension very slowly, and then, the vacuum Erlenmeyer flask was filled with deionized water. Then, the suspension was kept still for 48 h for the suspension to settle. In the tenth step, the suspension was filtered, and the filtrate was washed with deionized water and the pH was adjusted at 7.0. In the eleventh and twelfth steps, the materials were dried for 1 h at 100 ℃ in an oven and then placed in a humidity reduction chamber for 48 h. An overview of the steps can be seen in Fig. 1.

The GOPT nanocomposites were prepared by liquid/liquid interfacial polymerization as shown in Fig. 1 and described in Bora, *et al.* [20]. Compared to bulk polymerization, this method offers better control over surface topology and incorporation of functional groups [21]. In particular, this method facilitates the fabrication and deposition of thin polymer films on heterogeneous surfaces.

Characterization of Samples

The crystalline characteristics of the samples were evaluated using XRD analysis (D6792, Philips, Netherlands). The FTIR analysis was performed by Equinox 55 (Bruker, Germany) with 4 cm^{-1} resolution. pH was measured by a handheld pH meter (pH600, Milwaukee Instruments, Hungary). The concentration measurement was carried out by DR6000 UV-Vis spectrophotometer (Hack, United States). SEM (Model VEG, TESCAN, Czech Republic) at 3.0 kV was utilized for phase morphological analysis. The BET analysis was conducted using nitrogen adsorption/desorption.

Adsorption Experiments

Adsorption capacity and adsorption rate are important factors in assessment of adsorbents in practical applications, which provide the basis for process design, feasibility studies and economic analysis. In this study, different solutions containing various amounts of NB dye (10, 20, and 30 mg l^{-1}) were poured into a 50 ml volumetric flask along with 2 ml acetate buffer (pH = 5). Afterward, 0.1 g GOPT was added to each flask. Then, the resulting suspension was stirred for 150 s, and placed on a strong magnet to facilitate sedimentation. The light absorption of each sample was evaluated at $\lambda = 279$ nm.

The adsorption capacity (mg g^{-1}) and removal efficiency of NB is determined using the following expressions, respectively:

$$q = \frac{(C_0 - C_f)V}{M} \tag{1}$$

$$\text{Re}\,moval\ efficiency\ (\%) = \frac{C_0 - C_f}{C_0} \times 100 \tag{2}$$

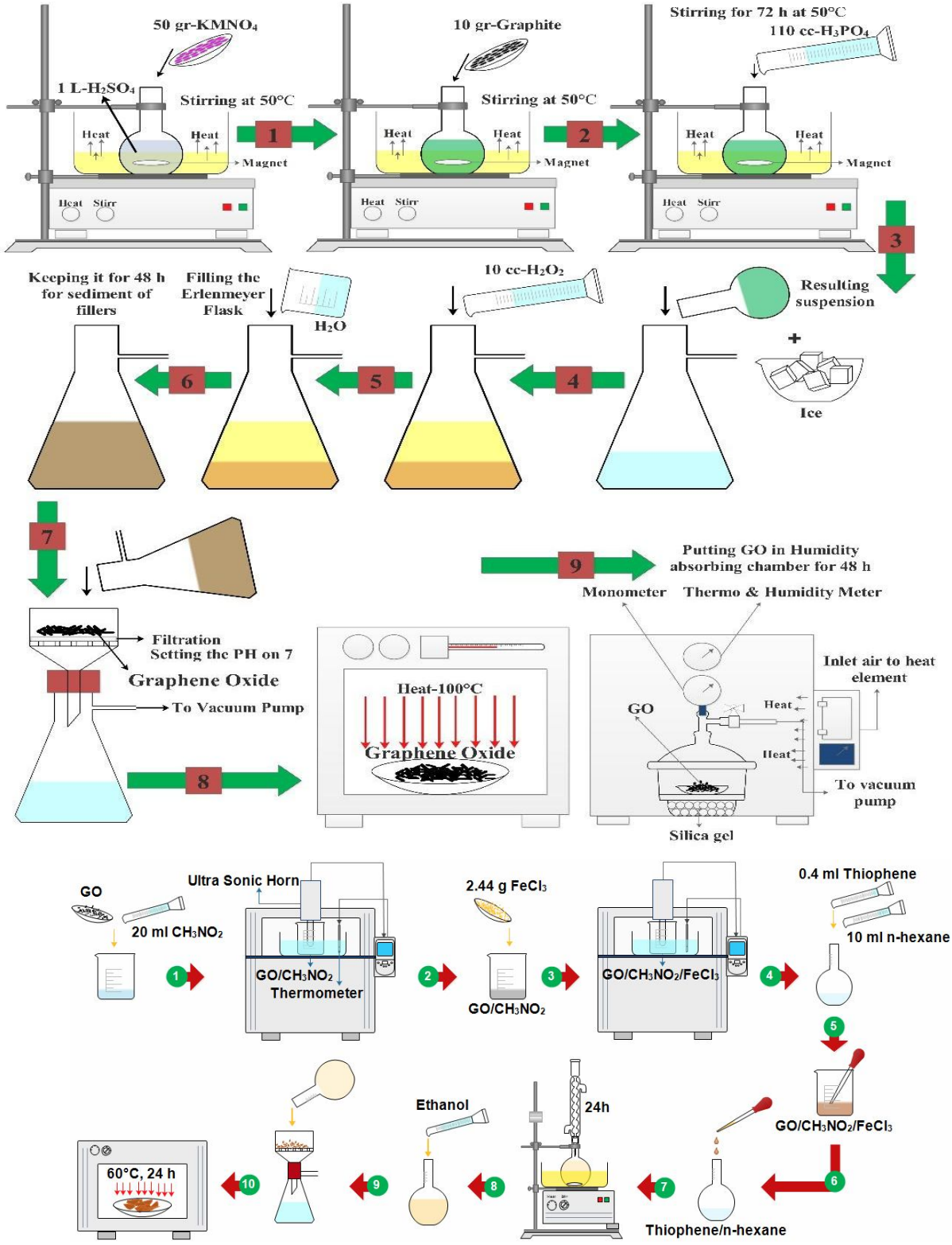

Fig. 1. GO and GOPT manufacturing processes.

where C_0 and C_f represent the initial and final concentrations, respectively. V is the volume of the solution (in ml) and M is the mass of adsorbent (in g). In the following paragraphs, q_t and q_e are used to denote adsorption capacity over time, and at equilibrium, respectively.

Samples of the NB solution were analyzed using a UV-Vis spectrophotometer at λ_{max} = 279 nm. All measurements were conducted in triplicates.

RESULTS AND DISCUSSION

XRD Analysis

X-ray diffraction (XRD) is the most widely used technique for general crystalline material characterization. It is used to measure the average spacing between layers or rows of atoms, and to determine the orientation of a single crystal or grain. For the synthesized GO nanoparticles obtained by the Hummer's method, the XRD pattern is shown in Fig. 2 and the inset within this figure. It shows the diffraction peak at 2θ = 10°, which is mainly due to the oxidation of graphite. Also, this peak can be attributed to the inter-planar distance between the GO sheets [22]. The diffraction peak of pure graphite is found at around 26°, corresponding to the highly organized layer structure with an interlayer distance of 0.34 nm along the (002) orientation, as also shown in Fig. 2.

FTIR Tests

Figure 3 compares the FTIR spectra of the materials under study. As can be seen in the FTIR spectrum of the undoped PT, the adsorption peaks at around 500 cm^{-1} and 750 cm^{-1} correspond to the bending mode of C-S and out-of-plane vibration of C-H bonds, respectively. The peak at about 1100 cm^{-1} can be assigned to the in-plane bending of C-H, while the peak around 1450 cm^{-1} indicates the C=C stretching within the aromatic ring. The peak at around 2900 is due to C=C-H stretching vibration mode in the aromatic ring, and the broad peak at about 3400 cm^{-1} corresponds to the O-H functional group. The presence of these peaks confirms the successful formation of PT [23].

The FTIR transmission spectrum of the product GOPT in Fig. 3 exhibits characteristic vibration at 29236.39 cm^{-1} for C-H stretching vibration band. The bands at 1688.20 and 1459.08 cm^{-1} correspond to C=C asymmetric and symmetric stretching vibrations of the thiophene ring, respectively. The vibration bands observed at 1290.29 cm^{-1} and 1068.70 cm^{-1} are due to C-H bending and the C-H in-plane deformation. Furthermore, the characteristic bands of PT are observed at 720.99 cm^{-1} (C-S bending) and 665.50 cm^{-1} (C-S-C ring deformation stretching), confirming the successful synthesis of GOPT nanocomposite. The slight shift toward the band at 3413.16 cm^{-1} originates from O-H [23]. It is worth noting that functional groups such as C=O, -OH, and -COOH from GO may contribute to the formation of active adsorbent sites [24]. Similarly, it can be concluded that the C-S group from PT acts as another type of adsorbent site, and since it is abundant in the molecular structure of the polymer, it has a significant effect on the adsorption capacity of the nanocomposite under study.

BET Analysis

The BET analysis offers quantitative insights into the surface properties of adsorbents. Using nitrogen adsorption, the specific surface area of GO was found to be 917.8 $m^2 g^{-1}$, with the adsorption average pore width calculated as 24.9 Å. The reported specific surface area is an obvious indicator of the large adsorption capacity of GO as the backbone of the synthesized GOPT nanocomposite.

SEM Analysis

SEM images shed light on some essential surface properties of nanocomposites, which contribute to their adsorption characteristics. Figures 4a and b show the SEM images of the neat GO samples at different magnifications. It is interesting to note that the surface structure of the synthesized samples is highly wrinkled compared to the results given in other studies [20,25]. While their synthesized GO sheets may be useful for good electrical properties due to surface smoothness, the samples prepared in this work are very suitable for adsorption systems as they offer a much higher interfacial surface area. The difference can be attributed to the variations in the details of fabrication procedure in particular ultrasonication and reaction under vacuum conditions. Based on the SEM results, the samples produced in this work are comparable with exfoliated graphene oxide reported elsewhere though obtained at elevated temperatures [26].

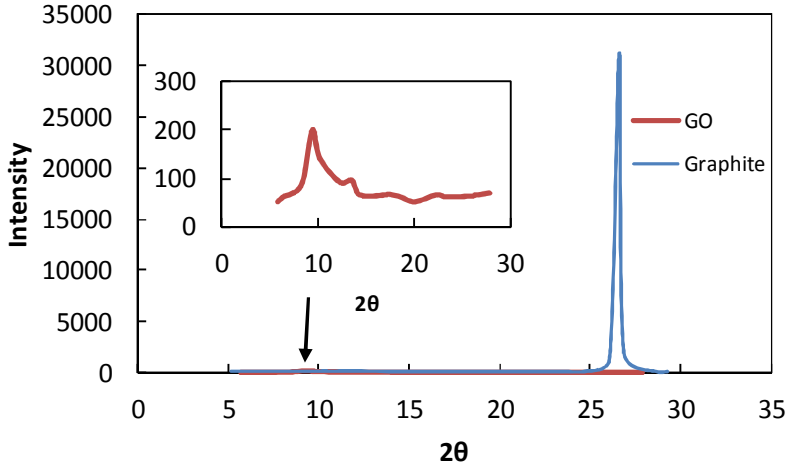

Fig. 2. XRD tests for graphene oxide (GO) and graphite.

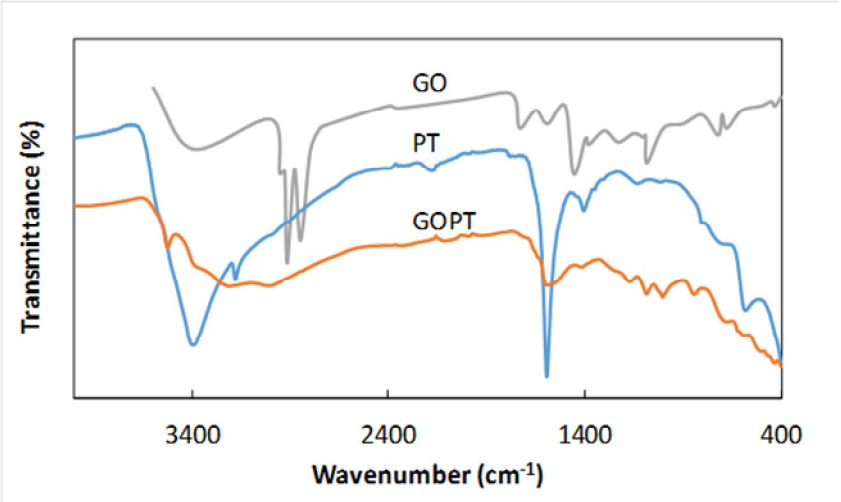

Fig. 3. FTIR tests: spectra of GO, PT and GOPT.

The SEM images of the fabricated GOPT nanocomposite are shown in Figs. 4c and d at different magnifications. As can be seen, the large surface area of the neat GO acts as an efficient support for the PT nanoparticles, while the suitable pore size helps in containing more dye molecules. Overall, the PT layer coated on the GO support visually offers a more porous morphology compared to the other studies [20,27], which is advantageous in applications involving adsorption of pollutants with a minimum mass of adsorbent. On the other hand, GO and PT crosslinks result in enhanced functionalization of PT compared with PT as the single adsorbent.

The Effect of Contact Time

The effect of contact time on the performance of GOPT in adsorbing NB was investigated in different concentrations. The solution pH and GOPT dosage were fixed at their obtained optimum values. Figure 5 shows the adsorption capacity of NB on GOPT as a function of time (in the range of 1-90 min). According to these results, the necessary stirring time for removing GOPT is 15 min. This

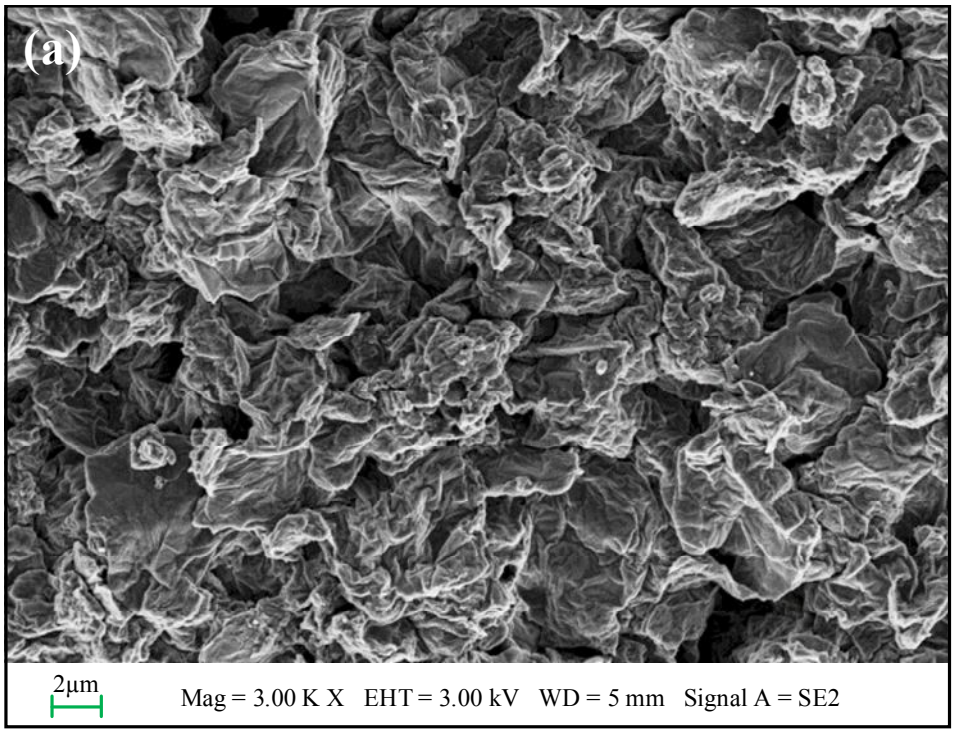

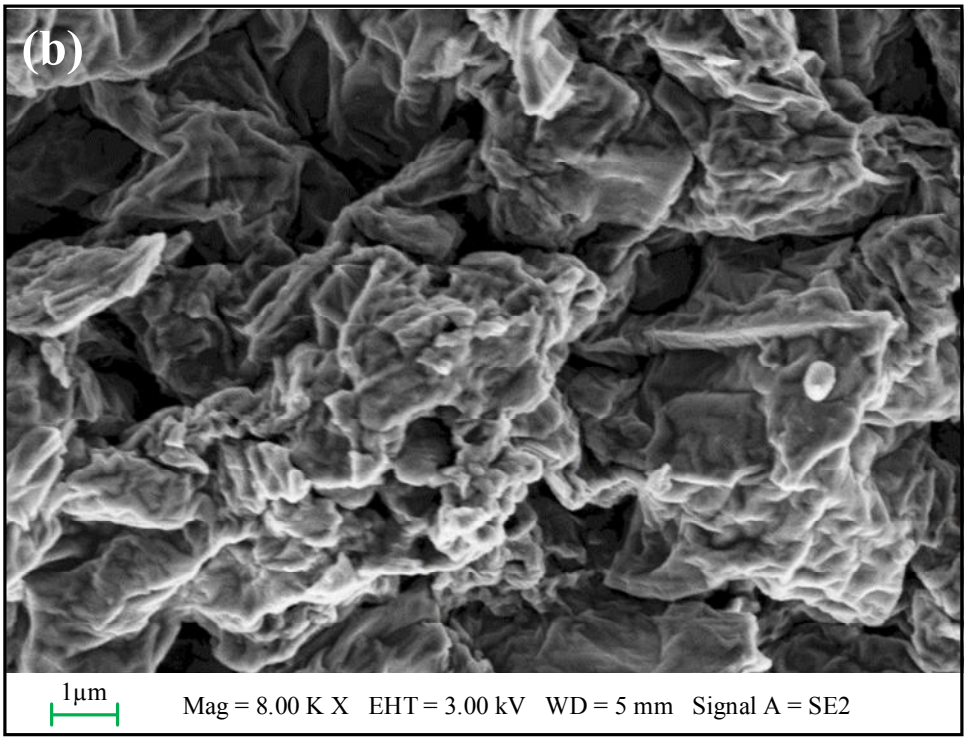

Fig. 4. SEM images of the samples: (a) and (b) GO alone, (c) and (d) GOPT nanocomposite.

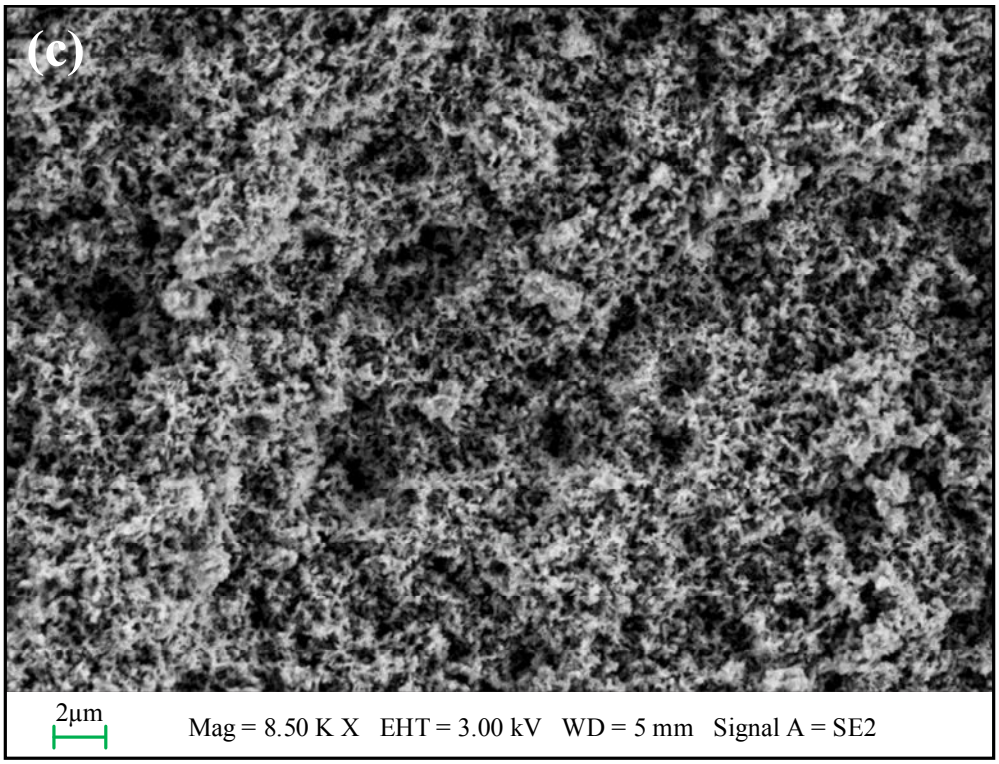

Fig. 4. Continued.

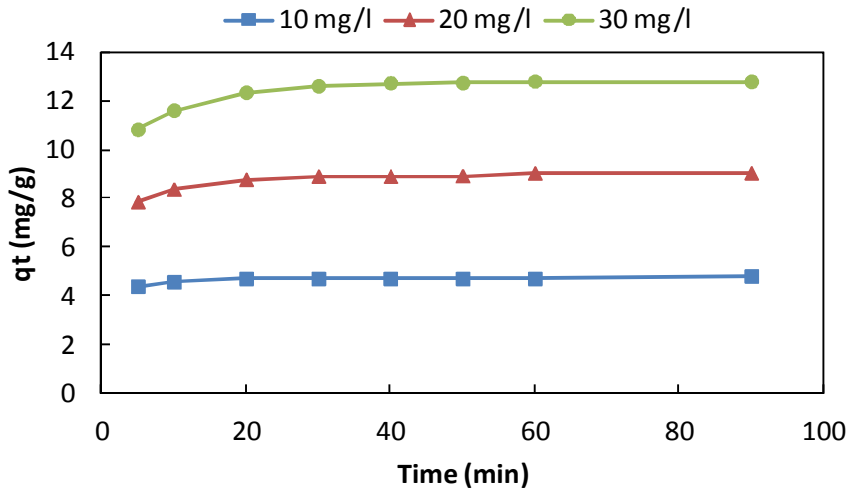

Fig. 5. Adsorption capacity *vs*. contact time for various initial NB concentrations.

data indicates that adsorption started immediately upon adding GOPT to the dye solution, indicating the absence of significant diffusional resistances. In fact, as suggested by Tamjidi *et al.* [28], the time-dependent adsorption process occurs in two stages; the first stage is fast as neither the diffusional resistances nor the repulsive forces from the adsorbed molecules are important. In the second stage however, these factors dominate the adsorption process as more vacant sites are occupied. These effects translate themselves into a much slower adsorption rate. Moreover, the adsorption rate is not a function of initial NB concentration as the equilibration time is almost equal for all experiments.

The removal efficiencies for the initial concentrations under study (10, 20 and 30 mg l^{-1}) can be readily calculated from this figure using Eq. (2), which are 52.0, 54.7 and 57.5%, respectively.

Adsorption Isotherms

In this section, the adsorption performance of the synthesized GOPT nanocomposite is described *via* isotherm determination. In this case, the distribution of the adsorbate between the liquid and the solid phases was examined using the Langmuir and Freundlich isotherm models via fitting the experimental data.

The Langmuir isotherm considers monolayer absorption over a uniform surface containing a finite number of identical adsorption sites, and besides, transmigration of the adsorbate molecules across the adsorbent sites is ignored. The Langmuir isotherm is defined in the linear form as follows:

$$\frac{C_e}{q_e} = \frac{1}{bq_{\max}} + \frac{C_e}{q_{\max}} \quad (3)$$

The constant b is the adsorption equilibrium constant, and q_{max} is the maximum adsorption capacity (number of active sites) per unit mass of adsorbent. The linear plot of the absorption specification (C_e/q_e) *vs*. the equilibrium concentration (C_e) can be seen in Fig. 6a from which the value of q_{max} is calculated as 15.6 mg g^{-1}. For the sake of comparison, the results of other studies on the adsorption of NB on various materials are summarized in Table 1. It is apparent that the adsorption capacity reported in this work is comparable to other studies.

Based on the linear plot given in Fig. 6a, the Langmuir isotherm model is relatively compatible with the experimental data (R^2 = 0.9825). The difference can be explained by the presence of different adsorption sites and also spatial limitations on the adsorbent surface, both contradicting the Langmuir assumptions, as discussed earlier. Of course, an R^2 value greater than 0.98 suggests that the adsorption is of monolayer nature, which is in accordance with the Langmuir assumptions [24].

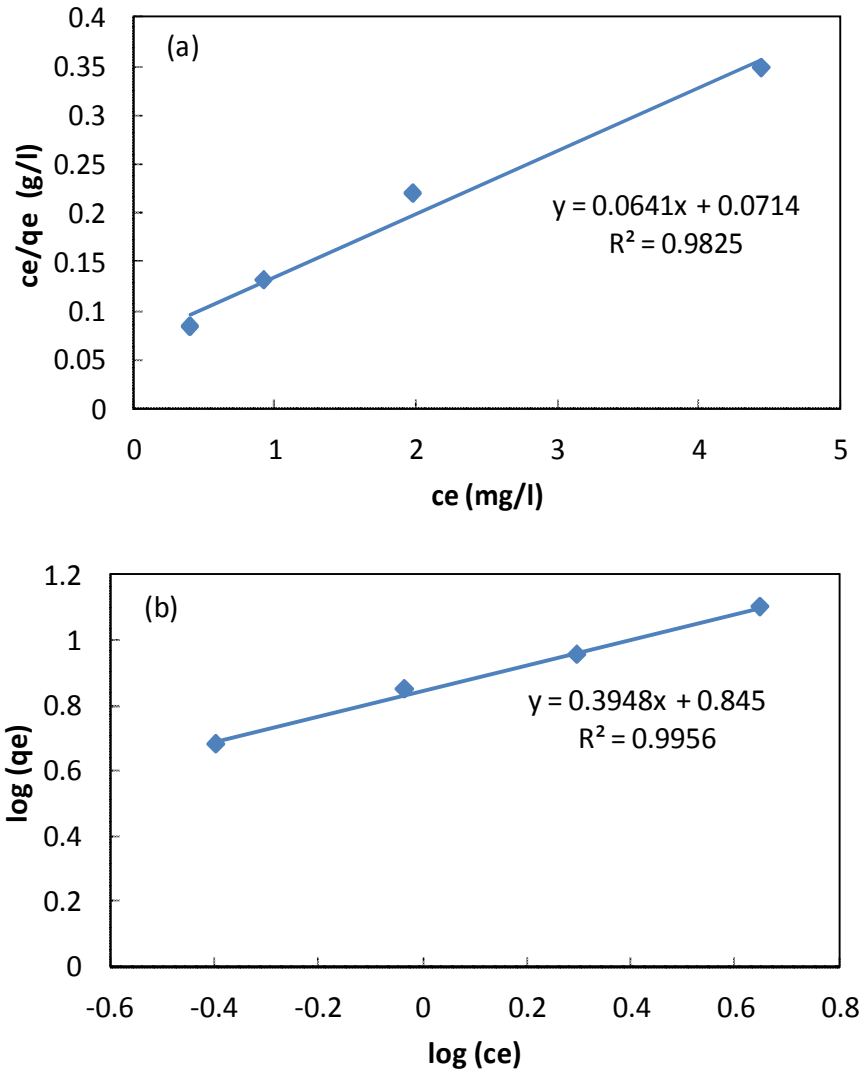

Fig. 6. Linear plots: (a) Langmuir isotherm, (b) Freundlich isotherm.

Table 1. Comparison of the Adsorption Capacity of Various Adsorbents for NB

Adsorbent	Temperature (°C)	Adsorption capacity (q_{max})	Ref.
GOPT	40	15.60	This work
Carbonized charring sugarcane bagasse	25	38.27	[24]
Nanocrystalline hydroxyapatite	25	8.993	[29]
Marine sediments	25	4.755	[30]
Wood-based activated carbon	25	263	[31]

On the other hand, the Freundlich isotherm is an empirical model, which can be defined in the linear form as follows:

$$\log q_e = \log K_f - \frac{1}{n}\log C_e \quad (4)$$

where K_f and n are the Freundlich constants based on the adsorption capacity and intensity, respectively. The Freundlich equilibrium constants can be determined from the plot of $\log q_e$ against $\log C_e$, which can be seen in Fig. 6b. We can observe that the experimental data complies better with the latter model based on a larger R^2 value ($R^2 = 0.9956$).

Kinetic Modeling of Adsorption

In the adsorption experiments, kinetic studies predict the adsorption rate and adsorption equilibrium time, which play important roles in the adsorption mechanism. Several models have been used to describe the adsorption kinetics. To describe the adsorption behavior and rate, the data obtained from the adsorption kinetic experiments were evaluated using pseudo-first-order and pseudo-second-order reaction rate models [20]. Figure 7 gives a summary of the regression results and R^2 values for the abovementioned models. According to the results, the dye adsorption process follows both pseudo-first order and pseudo-second-order models, though the pseudo-second-order model is more compatible with the experiments. This model indicates a chemical adsorption mechanism [24] which suggests electron sharing or transfer between the adsorbent and the adsorbate.

Effects of Initial pH

pH is an important factor affecting many adsorption systems. The protonation of functional groups is controlled by pH, and in ionic adsorption systems, this acts as an influential parameter [28]. However, since NB itself is not ionizable, it is unlikely that its adsorption mechanism is controled by protonation/deprotonation phenomena. Nevertheless, as can be seen in Fig. 8, the adsorption span at the range of 0.01-0.04 mg g^{-1}, indicating the significant effect of pH on the adsorption mechanism. Furthermore, the results show that the adsorption of NB on the prepared nanocomposite increased as the initial solution pH was changed from 3 to 5, and decreased after pH 5. Hence, the optimum value of the solution pH is 5, although moving to the neutral pH = 7 does not significantly reduce the adsorption capacity.

The effects of pH on the GO and hence its adsorption characteristics are complex, but one of the highly credited assumptions is the effect of pH on the GO colloidal particle size. It is worth noting that, as suggested by Kashyap, *et al.* [32], the GO colloidal particles have the minimum size at the pH range of 5-7, which is in good agreement with the maximum adsorption capacity as reported in our work.

Effects of Adsorbent Dosage

The study of the required adsorbent mass is useful for selecting an appropriate amount of adsorbent for industrial applications; note that equilibrium and kinetic studies may not accurately predict other practical limitations such as spatial inhibition whereas selecting the proper amount of adsorbent is also critical from the economic point of view. The effect of the adsorbent dosage on the NB removal was studied by varying the dosages of the nanocomposite from 0.05 to 0.13 g. The results are shown in Fig. 9. It is apparent that adsorption from the solution first increased with increasing adsorbent dosage to 0.1 g of adsorbent and decreased afterward. This can be explained as with increasing adsorbent dosage, more surface area is available for adsorption due to increase in the number of active sites to a certain extent [11]. However, after this point, the presence of more adsorbent may itself obstruct access to some distant sites and hence reduce adsorption efficiency [11].

Selection of Eluent (Regenerating Agent)

The nature and composition of eluent are of crucial importance. The best eluent is the one that elutes all of the retained adsorbates in a small volume. Four types of eluents namely, ammonia, ethanol, acetone, and sodium hydroxide were examined. Figure 10 presents the elution results, which indicates the advantage of polar eluents with respect to the others. The least retained amount belongs to sodium hydroxide, while the highest value is for ammonia.

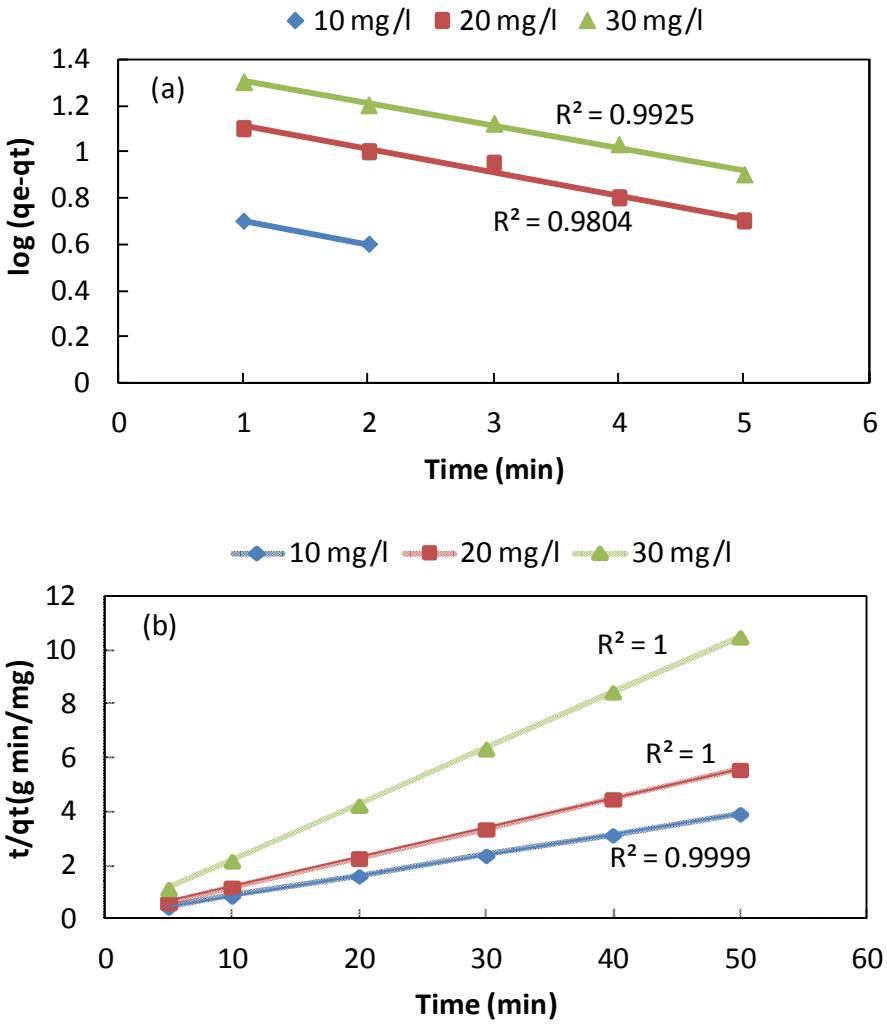

Fig. 7. (a) Pseudo-first-order kinetics, (b) Pseudo-second-order kinetic studies.

Regeneration of Adsorbent

In order to determine how many times a single column can be used for separation, four consecutive experiments were conducted on the same column. 1.0 ml of NB solution was added to the proper amount of distilled water, and after pH adjustment, the solution volume was brought to 100 ml. Then, the solution was passed at the flow rate of 9 ml min^{-1} through a column packed with 0.1 g of the composite adsorbent. The experiment was repeated for four consecutive runs. Based on the results, as given in Fig. 11, each column can be used for three times without a considerable loss of removal efficiency. In this figure, the efficiency is calculated with respect to the first adsorption cycle.

Effects of Temperature

In order to study the effects of temperature on the adsorption process of NB, experiments were conducted at 5 °C to 50 °C while other parameters were kept constant, as can be seen in Fig. 12. At first, adsorption increases as temperature is changed from 5 to 10 °C. However, beyond this range, from 10 to 25 °C, a drastic drop in adsorption is observed. Again from 25 to 40 °C, adsorption starts to rise, but beyond 40 °C and up to 50 °C, there is a slight reduction. Overall, maximum adsorption occurs at 40 °C.

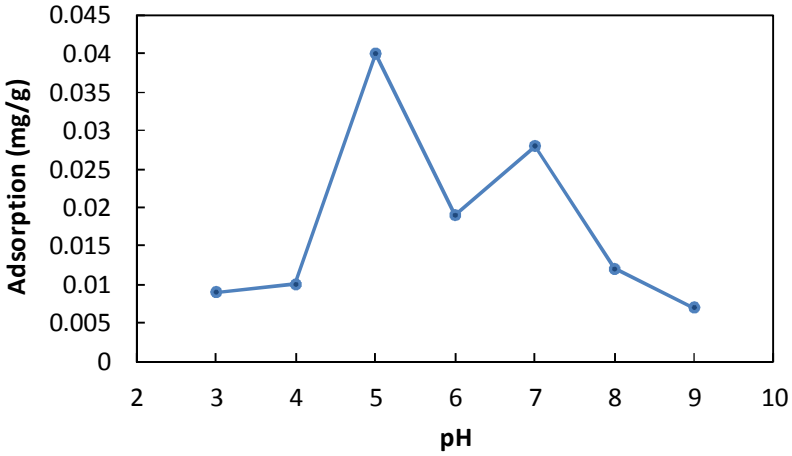

Fig. 8. Effects of initial pH on the adsorption capacity.

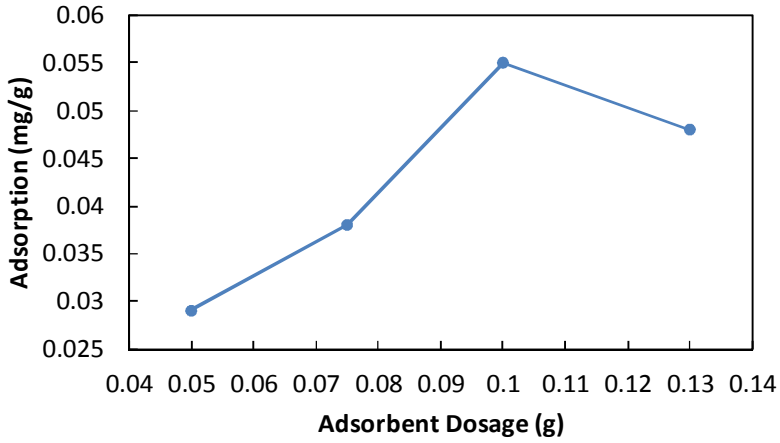

Fig. 9. Effects of adsorbent dosage.

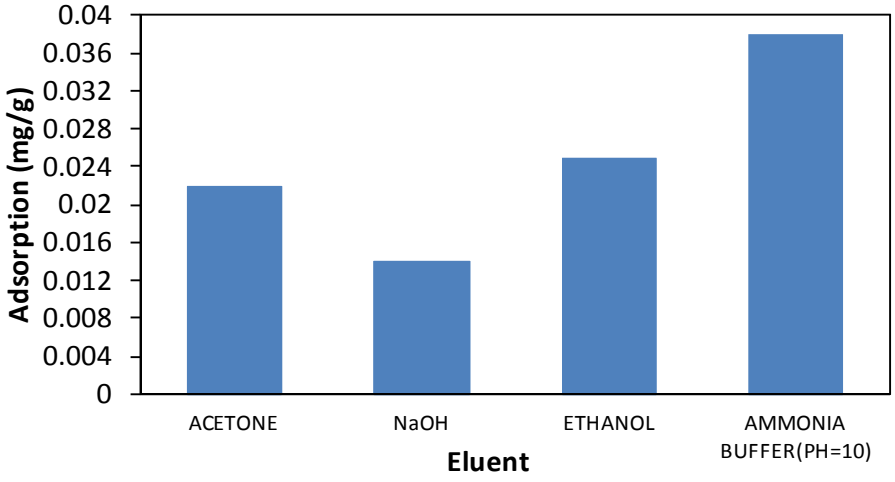

Fig. 10. Comparison of the eluents based on the elution capacity.

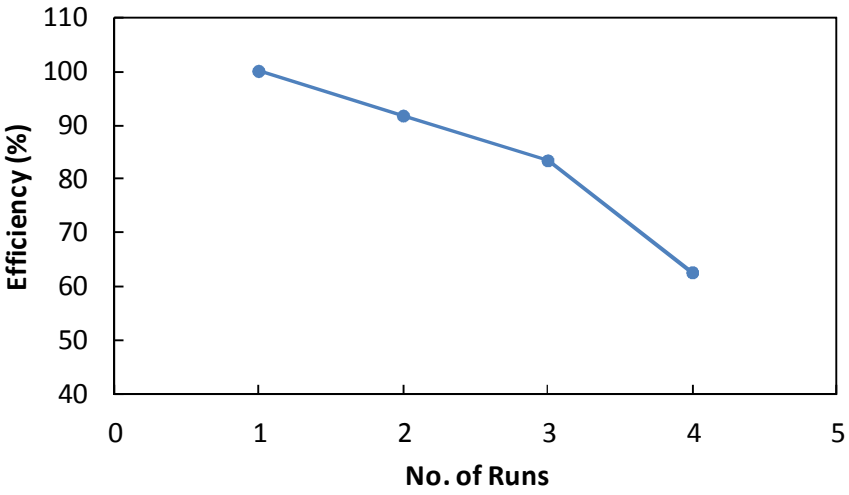

Fig. 11. Regeneration of adsorbent. Efficiency is calculated with respect to the first adsorption cycle.

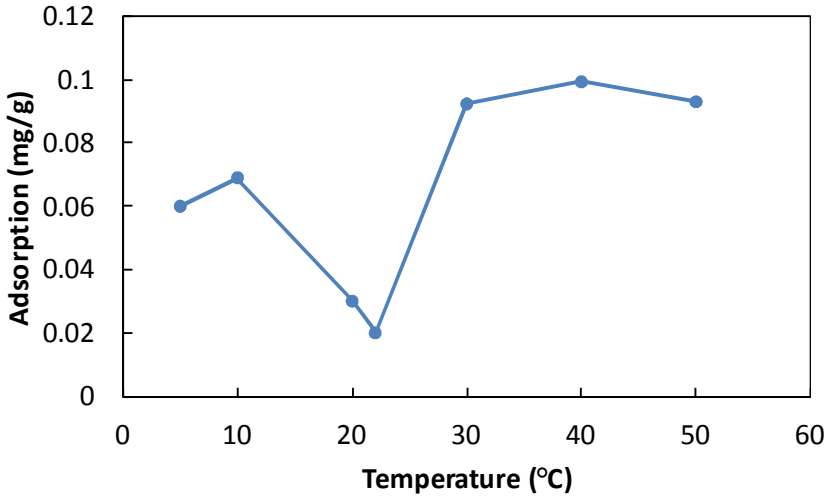

Fig. 12. Effects of temperature on adsorption.

CONCLUSIONS

The surface-modified nanocomposite adsorbent has been successfully synthesized by crosslinking graphene oxide (GO) with polythiophene (PT), which both possess multiple functionalities due to the presence of functional groups such as -OH, =CO, and sulfur.

With the method employed in this study, GO nanoparticles with relatively large surface area were produced. This characteristic makes them suitable for the adsorption systems either as the adsorbent or as the supporting structure. The addition of PT further modified the GO surface structure with suitable pore sizes for the adsorption of the NB dye molecules. This was reflected in the large adsorption capacity of the nanocomposite. Besides the SEM results, the XRD analysis clearly indicated the interaction of the GO nanoparticles with the PT emeraldine salt.

It must be emphasized that this novel adsorbent was produced from low-cost materials at relatively moderate

reaction conditions. It is also environmentally friendly with good dispersibility in water.

REFERENCES

[1] Mu, Y.; Rozendal, R. A.; Rabaey, K.; Keller, J., Nitrobenzene removal in bioelectrochemical systems. *Environ. Sci. Technol.,* **2009**, *43*, 8690-8695, DOI: 10.1021/es9020266.

[2] EPA, Toxicological Review of Nitrobenzene, U.S. Environmental Protection Agency Washington, D.C., 2009.

[3] Dong, J.; Zhao, Y.; Zhao, R.; Zhou, R., Effects of pH and particle size on kinetics of nitrobenzene reduction by zero-valent iron. *J. Environ. Sci.,* **2010**, *22*, 1741-1747, DOI: https://doi.org/10.1016/S1001-0742(09)60314-4.

[4] Liu, L.; Liu, S.; Zhang, Q.; Li, C.; Bao, C.; Liu, X.; Xiao, P., Adsorption of Au(III), Pd(II) and Pt(IV) from a solution onto graphene oxide. *J. Chem. Eng. Data,* **2013**, *58*, 209-216, DOI: 10.1021/je300551c.

[5] Qin, Q.; Xu, Y., Enhanced nitrobenzene adsorption in aqueous solution by surface silylated MCM-41. *Microporous Mesoporous Mater.,* **2016**, *232*, 143-150, DOI: https://doi.org/10.1016/j.micromeso.2016.06.018.

[6] Sun, Y.; Yang, S.; Zhao, G.; Wang, Q.; Wang, X., Adsorption of polycyclic aromatic hydrocarbons on graphene oxides and reduced graphene oxides. *Chem. Asian J.,* **2013**, *8*, 2755-2761, DOI: DOI: 10.1002/asia.201300496.

[7] Chen, W.; Duan, L.; Zhu, D., Adsorption of polar and nonpolar organic chemicals to carbon nanotubes. *Environ. Sci. Technol.,* **2007**, *41*, 8295-8300, DOI: 10.1021/es071230h.

[8] Foroutan, R.; Mohammadi, R.; Farjadfard, S.; Esmaeili, H.; Saberi, M.; Sahebi, S.; Dobaradaran, S.; Ramavandi, B., Characteristics and performance of Cd, Ni, Pb bio-adsorption using Callinectes sapidus biomass: real wastewater treatment. *Environ. Sci. Pollut. Res.,* **2019**, *26*, 6336-6347, DOI: 10.1007/s11356-018-04108-8.

[9] Tamjidi, S.; Esmaeili, H.; Kamyab Moghadas, B., Application of magnetic adsorbents for removal of heavy metals from wastewater: a review study. *Mater. Res. Express,* **2019**, *6*, 102004, DOI: 10.1088/2053-1591/ab3ffb.

[10] Abshirini, Y.; Esmaeili, H.; Foroutan, R., Enhancement removal of Cr(VI) ion using magnetically modified MgO nanoparticles. *Mater. Res. Express,* **2019**, *6*, 125513, DOI: 10.1088/2053-1591/ab56ea.

[11] Shi, H.; Li, W.; Zhong, L.; Xu, C., Methylene blue adsorption from aqueous solution by magnetic cellulose/graphene oxide composite: Equilibrium, kinetics, and thermodynamics. *Ind. Eng. Chem. Res.,* **2014**, *53*, 1108-1118, DOI: 10.1021/ie4027154.

[12] Salari, H.; Daliri, A.; Gholami, M. R., Graphitic carbon nitride/reduced graphene oxide/silver oxide nanostructures with enhanced photocatalytic activity in visible light. *Phys. Chem. Res.,* **2018**, *6*, 729-740, DOI: 10.22036/pcr.2018.137083.1501.

[13] Hansora, D. P.; Shimpi, N. G.; Mishra, S., Graphite to graphene *via* graphene oxide: An overview on synthesis, properties and applications. *JOM,* **2015**, *67*, 2855-2868, DOI: 10.1007/s11837-015-1522-5.

[14] Ramesha, G. K.; Vijaya Kumara, A.; Muralidhara, H. B.; Sampath, S., Graphene and graphene oxide as effective adsorbents toward anionic and cationic dyes. *J. Colloid Interface Sci.,* **2011**, *361*, 270-277, DOI: https://doi.org/10.1016/j.jcis.2011.05.050.

[15] Yu, L.; Wang, L.; Xu, W.; Chen, L.; Fu, M.; Wu, J.; Ye, D., Adsorption of VOCs on reduced graphene oxide. *J. Environ. Sci.,* **2018**, *67*, 171-178, DOI: https://doi.org/10.1016/j.jes.2017.08.022.

[16] Kim, M.; Lee, C.; Seo, Y. D.; Cho, S.; Kim, J.; Lee, G.; Kim, Y. K.; Jang, J., Fabrication of various conducting polymers using graphene oxide as a chemical oxidant. *Chem. Mater.,* **2015**, *27*, 6238-6248, DOI: 10.1021/acs.chemmater.5b01408.

[17] Wu, T.; Cai, X.; Tan, S.; Li, H.; Liu, J., Yang, W., Adsorption characteristics of acrylonitrile, *p*-toluenesulfonic acid, 1-naphthalenesulfonic acid and methyl blue on graphene in aqueous solutions. *Chem. Eng. J.,* **2011**, *173*, 144-149, DOI: https://doi.org/10.1016/j.cej.2011.07.050.

[18] Chaudhary, R. P.; Pawar, P. B.; Vaibhav, K.; Saxena, S.; Shukla, S., Quantification of adsorption of Azo

dye molecules on graphene oxide using optical spectroscopy. JOM, **2017**, 69, 236-240, DOI: 10.1007/s11837-016-2172-y.

[19] Ansari, M. O.; Khan, M. M.; Ansari, S. A.; Cho, M. H., Polythiophene nanocomposites for photodegradation applications: Past, present and future. *J. Saudi Chem. Soc.,* **2015**, *19*, 494-504, DOI: https://doi.org/10.1016/j.jscs.2015.06.004.

[20] Bora, C.; Pegu, R.; Saikia, B.J.; Dolui, S. K., Synthesis of polythiophene/graphene oxide composites by interfacial polymerization and evaluation of their electrical and electrochemical properties. *Polym. Int.,* **2014**, *63*, 2061-2067, DOI: 10.1002/pi.4739.

[21] Song, Y., Fan, J. -B., Wang, S., Recent progress in interfacial polymerization. *Mater. Chem. Front.,* **2017**, *1*, 1028-1040, DOI: 10.1039/c6qm00325g.

[22] Molaei, K.; Bagheri, H.; Asgharinezhad, A. A.; Ebrahimzadeh, H.; Shamsipur, M., SiO_2-coated magnetic graphene oxide modified with polypyrrole-polythiophene: A novel and efficient nanocomposite for solid phase extraction of trace amounts of heavy metals. *Talanta,* **2017**, *167*, 607-616, DOI: https://doi.org/10.1016/j.talanta.2017.02.066.

[23] Chen, X.; Chen, B., Macroscopic and spectroscopic investigations of the adsorption of nitroaromatic compounds on graphene oxide, reduced graphene oxide, and graphene nanosheets. *Environ. Sci. Technol.,* **2015**, *49*, 6181-6189, DOI: 10.1021/es5054946.

[24] Wang, D.; Shan, H.; Sun, X.; Zhang, H.; Wu, Y., Removal of nitrobenzene from aqueous solution by adsorption onto carbonized sugarcane bagasse. *Adsorpt. Sci. Technol.,* **2018**, *36*, 13661385, DOI: https://doi.org/10.1177/0263617418771823.

[25] Zhang, L. L.; Zhao, S.; Tian, X. N.; Zhao, X. S., Layered graphene oxide nanostructures with sandwiched conducting polymers as supercapacitor electrodes. *Langmuir,* **2010**, *26*, 17624-17628, DOI: 10.1021/la103413s.

[26] Kumar, V.; Kumar, A.; Bhandari, S.; Biradar, A. M.; Reddy, G. B.; Pasricha, R., Exfoliation of graphene oxide and its application in improving the electro-optical response of ferroelectric liquid crystal. *J. Appl. Phys.,* **2015**, *118*, 114904, DOI: 10.1063/1.4930949.

[27] Mishra, A. K.; Agrawal, N. R.; Das, I., Synthesis of water dispersible dendritic amino acid modified polythiophenes as highly effective adsorbent for removal of methylene blue. *J. Environ. Chem. Eng.,* **2017**, *5*, 4923-4936, DOI: https://doi.org/10.1016/j.jece.2017.09.017.

[28] Tamjidi, S.; Esmaeili, H., Chemically modified CaO/Fe_3O_4 nanocomposite by sodium dodecyl sulfate for Cr(III) removal from water. *Chem. Eng. Technol.,* **2019**, *42*, 607-616, DOI: 10.1002/ceat.201800488.

[29] Wei, W.; Sun, R.; Cui, J.; Wei, Z., Removal of nitrobenzene from aqueous solution by adsorption on nanocrystalline hydroxyapatite. *Desalination,* **2010**, *263*, 89-96, DOI: https://doi.org/10.1016/j.desal.2010.06.043.

[30] Zhao, X. -K.; Yang, G. -P.; Gao, X. -C., Studies on the sorption behaviors of nitrobenzene on marine sediments. *Chemosphere,* **2003**, *52*, 917-925, DOI: https://doi.org/10.1016/S0045-6535(03)00258-3.

[31] Dai, Y.; Mihara, Y.; Tanaka, S.; Watanabe, K.; Terui, N., Nitrobenzene-adsorption capacity of carbon materials released during the combustion of woody biomass. *J. Hazard. Mater.,* **2010**, *174*, 776-781, DOI: https://doi.org/10.1016/j.jhazmat.2009.09.119.

[32] Kashyap, S.; Mishra, S.; Behera, S. K., Aqueous colloidal stability of graphene oxide and chemically converted graphene. *J. Nanopart.,* **2014**, *2014*, 6, DOI: 10.1155/2014/640281.